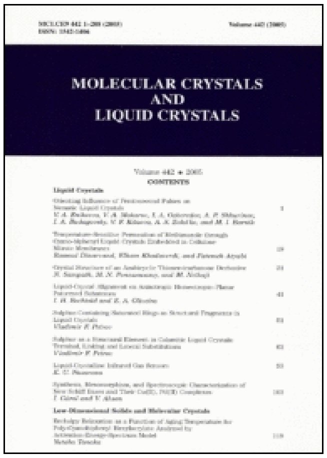

Molecular Crystals and Liquid Crystals

Publication details, including instructions for authors and subscription information:
http://www.informaworld.com/smpp/title~content=t713644168

Electro-Optic Characteristics of Single Gap Transflective Display Using In-Plane Switching Mode

Je Hoon Song [a]; Seung Hee Lee [a]; Do Sung Kim [b]; Hoe-Sub Soh [b]; Woo Yeol Kim [b]

[a] School of Advanced Materials Engineering, Chonbuk National University, Chonju-si, Chonbuk, Korea
[b] Advanced Technology Development Team, LG-Philips LCD, Kumi-si, Kyungbuk, Korea

Online Publication Date: 01 June 2005
To cite this Article: Song, Je Hoon, Lee, Seung Hee, Kim, Do Sung, Soh, Hoe-Sub and Kim, Woo Yeol (2005) 'Electro-Optic Characteristics of Single Gap Transflective Display Using In-Plane Switching Mode', Molecular Crystals and Liquid Crystals, 433:1, 105 - 115
To link to this article: DOI: 10.1080/15421400590955505
URL: http://dx.doi.org/10.1080/15421400590955505

Mol. Cryst. Liq. Cryst., Vol. 433, pp. 105–115, 2005
Copyright © Taylor & Francis Inc.
ISSN: 1542-1406 print/1563-5287 online
DOI: 10.1080/15421400590955505

Electro-Optic Characteristics of Single Gap Transflective Display Using In-Plane Switching Mode

Je Hoon Song
Seung Hee Lee
School of Advanced Materials Engineering, Chonbuk National University, Chonju-si, Chonbuk, Korea

Do Sung Kim
Hoe-Sub Soh
Woo Yeol Kim
Advanced Technology Development Team, LG-Philips LCD, Kumi-si, Kyungbuk, Korea

We have designed a single gap transflective liquid crystal display (LCD) using an in-plane switching mode, where the rotating angle of the LC director between electrodes, and above electrodes, is 45° and 22.5° in average, respectively. Optimization of the cell structures such as electrode structure, cell structure, physical properties of the LC and the LC cell retardation value have been perform to obtain a low-power transflective LCD with a single gap structure and a single driving circuit.

Keywords: in-plane switching; single driving circuit; single gap transflective LCD

INTRODUCTION

Recently, reflective LCDs are used for many mobile applications, since reflective LCDs have many advantages, such as low power consumption, lightweight, and good reliability for outdoor use. However, reflective LCDs are not always convenient when they are used indoors. In order to improve the legibility, not only outdoors, but also indoors, transflective LCDs have recently been developed [1].

This work was supported by grant No. R01-2004-000-10014-0 from the Basic Research program of the Korea Science & Engineering Foundation and in part by LC-Philips project.

Address correspondence to Seung Hee Lee, School of Advanced Materials Engineering, Chonbuk National University, Chonju-si, Chonbuk, 561-756, Korea. E-mail: lsh1@chonbuk.ac.kr

In general, the design of the transflective LCD is classified into two cases. One is the dual cell gap structure [2–4] and the other is a singe gap transflective display using a multi-driving circuit [5]. In the dual gap structure, a cell gap in the transmissive part is twice that of a reflective part, and thus in comparison to the reflective LCD, the fabrication process is relatively complex. For a transflective display using multi-driving circuit, a single cell gap is used, however, the cost of circuit parts increases.

Various LC cell designs, such as in-plane switching (IPS) [6], multi-domain-vertical-alignment (MVA) [7], optically compensated bend (OCB) [8], and fringe-field switching (FFS) [9] modes with a wide viewing angle, have been commercialized for relatively large size transmissive displays, however, nowadays they are even being applied to small size transmissive displays, although the devices are not effective in power consumption.

Among them, the IPS mode in which the LC director rotates in plane, was applied to a single gap transflective display [10]. In the device, the electrode width (w) and the distance between the electrodes (l) strongly affected the electro-optic characteristics of the cells, such as reflectance (R), transmittance (T), operating voltage (V_{op}) and response time. Furthermore, the device requires a high operating voltage, which is not effective for mobile display uses. Therefore, we investigated a low driving single-gap transflective display by optimizing electrode structure, cell structure and LC physical properties.

CELL STRUCTURE AND SWITCHING PRINCIPLE

The cell structure of the proposed single gap transflective LCD is shown in Figure 1. In the device, the pixel and counter electrodes, which are opaque metals that play the role of a reflector, exist only on the bottom substrate. The in-cell retarder with a quarter-wave plate ($\lambda/4$) exists above the electrodes. A compensation film of $\lambda/4$ exists below the substrate. Two polarizers are crossed to each other, and an optic axis of the LC coincides with one of the polarizer axes. As indicated in Figure 1, with applied voltage, a horizontal field is generated and thus, the LC rotates in plane. However, the twist angle of the LC director between and above electrodes differ from each other due to different dielectric torques in different positions, such that the twist angle of the LC director above electrode is lower than that between electrodes. Utilizing this concept, it is possible to design the transflective LCD with a single cell gap and single driving circuit [10].

Figure 2 reveals an optical cell configuration for both the reflective and transmissive areas in the proposed transflective IPS cell. Here,

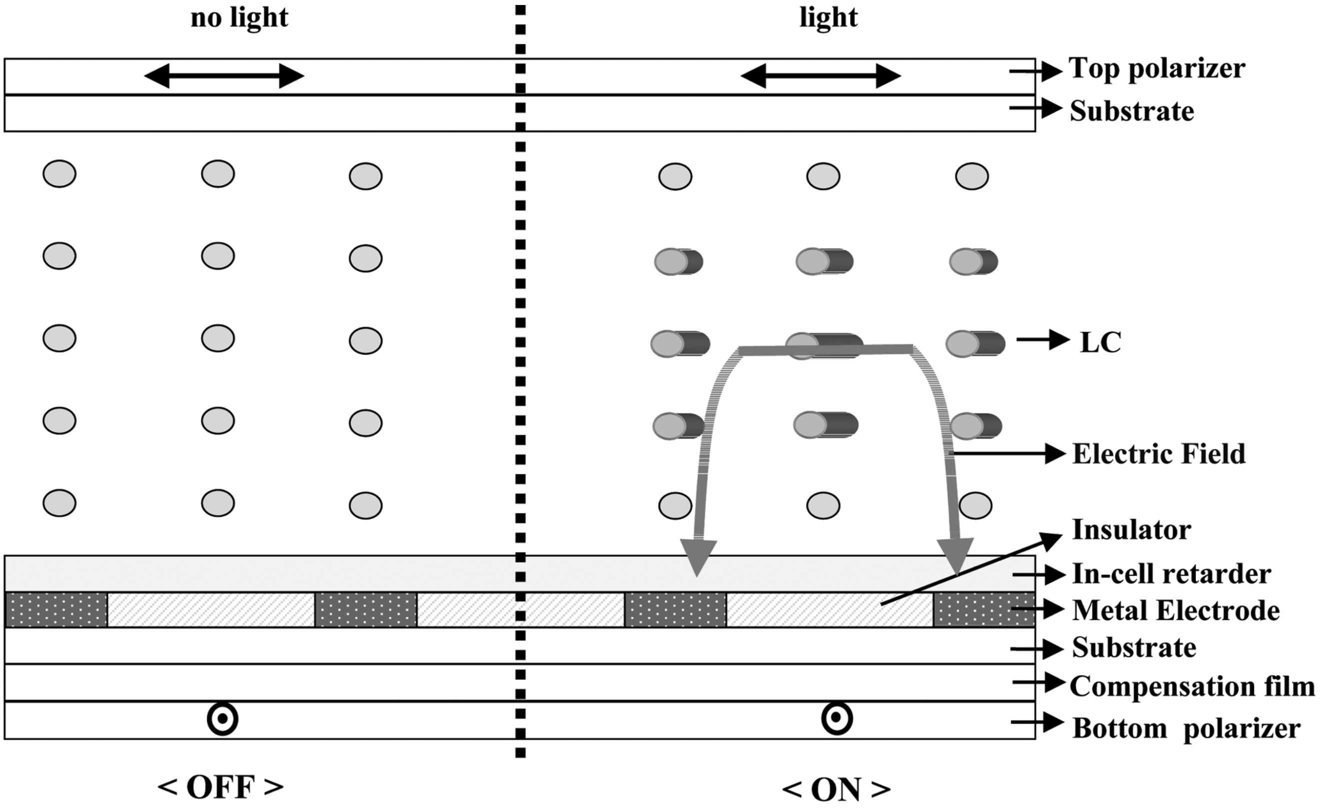

FIGURE 1 Schematic cell structure of the in-plane switching driven transflective LCD in the on and off states.

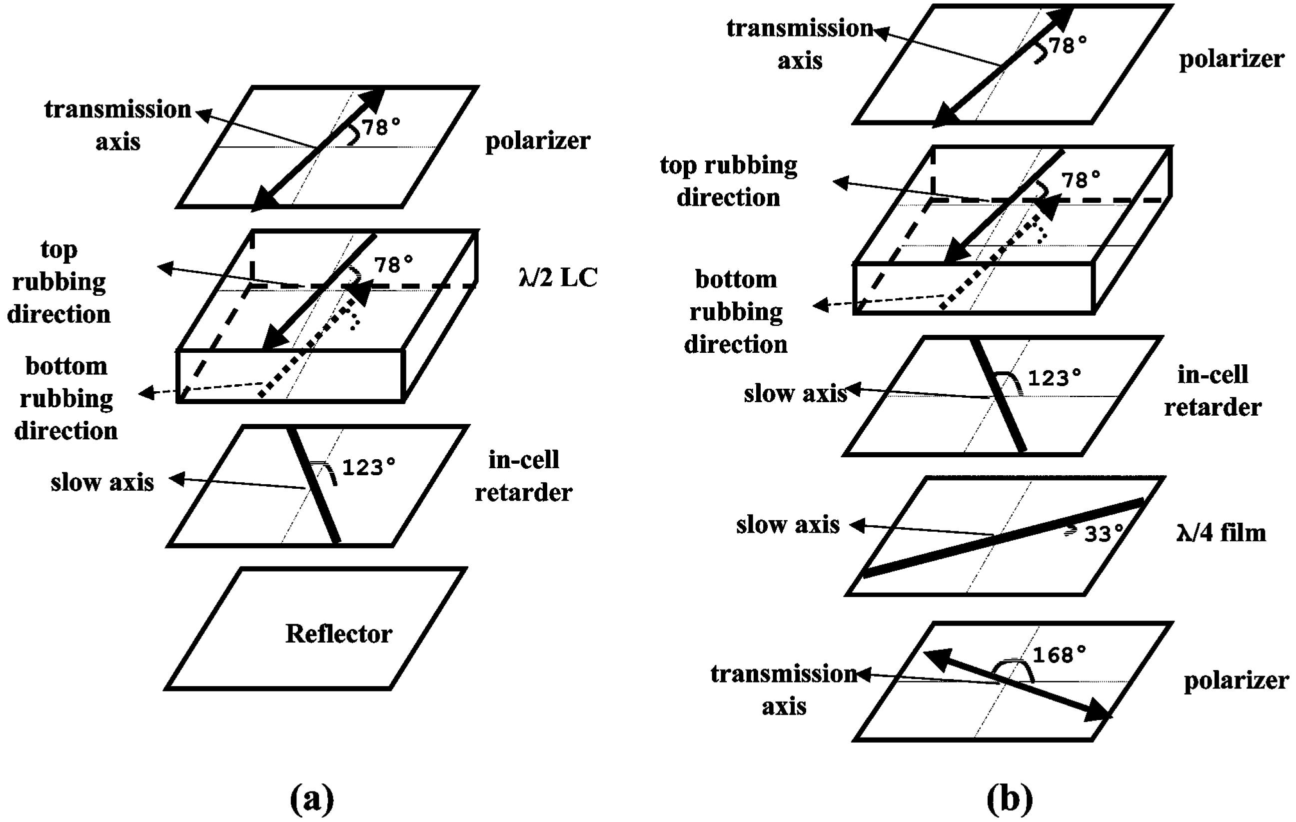

FIGURE 2 Optical cell configurations of the (a) reflective and (b) transmissive areas.

the area above the electrodes is used as the reflective area, whereas the area between the electrodes is used as the transmissive area. In the reflective area, the polarizer axis and the LC axis coincide with one another, and below the LC layer, the $\lambda/4$ in-cell retarder with slow axis making 45° with the LC optic axis is used. The electrode plays the role of a reflector. In the off state, the linearly polarized light simply passes through the LC layer, without a change in polarization, and becomes circularly polarized after the retarder of $\lambda/4$. After reflection, it propagates along the retarder and the LC layer again, and becomes linearly polarized and rotated by 90°. After this, the cell appears to be black. In the on state, the LC directors are rotated about 22.5° by the in-plane field. Then, the linearly polarized light changes to a 45° direction, since the effective cell retardation value ($d\Delta n$) is assumed to be $\lambda/2$, and it propagates along a slow axis of the retarder, without changing its polarization state. This light passes the LC cell again and afterwards the vibration direction equal to the polarizer axis direction, which results in a bright state. In the transmissive area, with use of a non-patterned retarder under crossed polarizers, a compensation film of $\lambda/4$ with an optic axis of 90° with the slow axis of the in-cell retarder, is used below the substrate to cancel the phase generated by the retarder. In the off state, the linearly polarized light passes through the film so that it becomes circularly polarized. Next, this circularly polarized light passes through the in-cell retarder, and it becomes a linearly polarized light, after returning to its original polarization state. Finally, this light propagates along the LC layer without changing in its polarization state. Thus it is blocked by analyzer, which results in a dark state. With a bias voltage, the LC directors rotate by 45° so that the input light is rotated 90°, which results in a bright state.

RESULTS AND DISCUSSION

In the IPS cell, the electro-optic characteristics, in particular the R, T and V_{op}, depend on the ratio l and w since a change in the area ratio between transmissive and reflective areas causes different twist angles in reflective and transmissive areas. The V_{op} of the IPS cell is governed by $\pi l/d\ (k_2/\Delta\varepsilon)^{1/2}$, where d is a cell gap and $\Delta\varepsilon$ is dielectric anisotropy. Therefore, to control the V_{op}, the optimization of l, d, and $\Delta\varepsilon$ should be performed. Furthermore, in the IPS mode, the rubbing angle also affects the V_{op} so that it is also studied [11]. For reflectance and transmittance, the light intensity can be described as

$$R = \eta_{\mathrm{w}}(w) \times w; \quad T = \eta_{\mathrm{l}}(l) \times l \tag{1}$$

where η_w is electrode position dependent-light efficiency above electrode and η_l is electrode position dependent-light efficiency between electrodes. Hereafter, the R and the T value indicate the average value in the reflective and transmissive areas. Therefore, in order to achieve in-plan field driven single gap transflective display with high light efficiency, low driving voltage, and the same V_{op} in the reflective and transmissive areas, we investigated the R, the T and the V_{op} as a function of w and l through simulation.

To optimize electro-optic characteristics of the proposed transflective LCD, a simulation was performed by LCD master (Shintech, Japan) and an optical calculation was based on the 2×2 extended Jones matrix methods [12]. For the simulation, the thickness of in-cell retarder is 1.8 μm and the thickness of the LC layer (d) is 4 μm. Here, the elastic constant of the LC, K_1 (splay), K_2 (twist) and K_3 (bend) are 11.7 pN, 5.1 pN and 16.1 pN, respectively. The dielectric anisotropy ($\Delta\varepsilon$) of the LC is 7.4. The surface tilt angle of the LC is 2° with an initial rubbing direction of 78° with respect to its horizontal field. The cell retardation value ($d\Delta n$) was varied to determine an optimal value by changing birefringence (Δn) of the LC. For calculations, the transmittances for the single and parallel polarizers were assumed to be 41% and 35%, respectively.

Table 1 indicates calculated results for maximal R and T, and V_{op} for each condition in the single gap transflective IPS cell. Here, the $d\Delta n$ values are ones when the V_{op}s are the same each other in reflective and transmissive areas. As indicated, when the areas of w and l change, the R, T, V_{op} and optimal $d\Delta n$ value for maximal light efficiency change. The results indicate that the $d\Delta n$ value showing the same V_{op}s in the reflective and transmissive areas for a single driving circuit slightly increases as l for given w. For example, when

TABLE 1 The Optimal $d\Delta n$, R_{max}, T_{max} and V_{op} as a Function of the w and l

w:l (μm)	$d\Delta n$ (μm)	R_{max} (%)	T_{max} (%)	V_{op} (V)
4:7	0.28	32.94	30.38	6.5
4:8	0.30	32.76	31.84	6.6
5:7	0.28	31.68	30.92	6.1
5:8	0.30	31.37	32.34	6.3
5:9	0.32	31.10	33.26	6.4
5:10	0.32	30.86	33.75	6.7
6:7	0.30	29.85	32.78	5.7
6:8	0.30	29.79	32.67	6.0
6:9	0.32	29.41	33.55	6.2

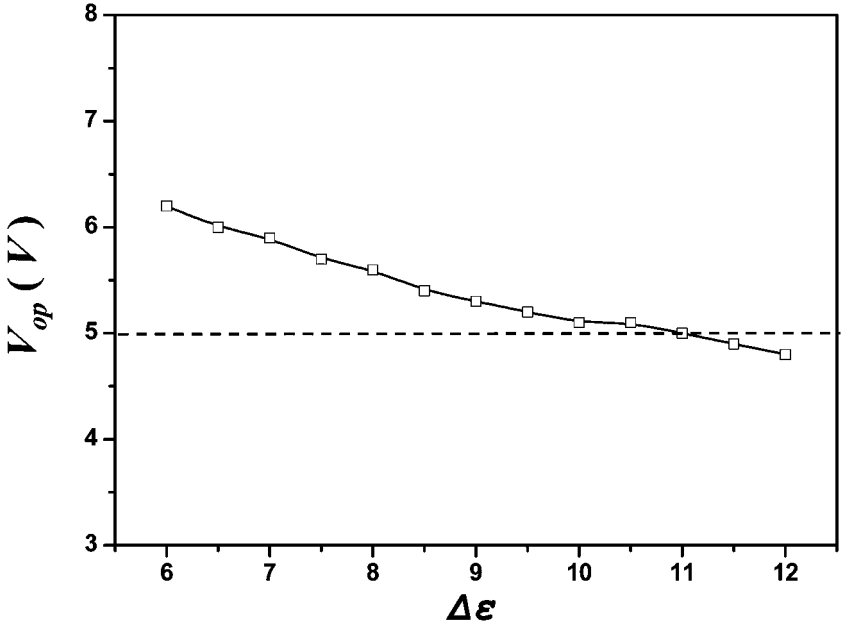

FIGURE 3 Operation voltage dependent on the dielectric anisotropy of the LC when w and l are 6 μm and 7 μm, respectively.

the w and l is 5 μm and 10 μm it is 0.32 μm, compared to the 0.28 μm when w and l is 5 μm and 7 μm. However, the R decreases with increasing l and w. For the V_{op}, it increases with increasing l but decreases with increasing w. For mobile displays, a low V_{op} is highly important for low power consumption. Thus, from the viewpoint of V_{op}, it shows the lowest value of 5.7 V when the w and l is 6 μm and 7 μm, respectively. In addition to this, we found that if the w is larger or equal to the l, the $d\Delta n$ value showing the same V_{op} in the reflective and transmissive areas does not exist. Also, if the ratio l to w is larger than 2, the same V_{op}s for the reflective and transmissive areas occur at a very high voltage, which is not favorable for mobile transflective displays. To lower the V_{op} of the single gap in-plane field driven transflective display below 5 V, when the w and l is 6 μm and 7 μm, we calculated the V_{op} as a function of $\Delta\varepsilon$, as shown in Figure 3. The result demonstrates that low-power transflective LCD like 5 V can be obtained if a LC material with $\Delta\varepsilon$ value is more than 11. Since the V_{op} is also dependent on the rubbing angle, the maximal R and T, and V_{op} as a function of rubbing angles when $\Delta\varepsilon$ value of the LC is 11 is calculated, as shown in Table 2. As indicated, as the rubbing angle increases from

TABLE 2 The $R_{\max}$, $T_{\max}$ and V_{op} as a Function of the Rubbing Angles

Rubbing angles (deg.)	$R_{\max}$ (%)	$T_{\max}$ (%)	V_{op} (V)
78	29.50	32.71	5.0
83	29.66	32.66	4.8

78° to 83°, the V_{op} decreases by 0.2 V, and the transmittance and reflectance slightly changes such that the reflectance increases slightly due to increased twist angle above electrodes, however, the difference is minimal [13]. This implies that for the mobile display with low driving voltage and high light efficiency, a large rubbing angle is more favorable. Next, the V_{op} is calculated as a function of the thickness of the in-cell retarder. In general, the thickness of the film to have a quarter-wave plate can be varied depending on process condition [14]. When it decreases from 1.8 μm to 0.9 μm, the V_{op} drops to 4.4 V from 4.8 V, as shown in Figure 4. Therefore, reducing the thickness of the in-cell retarder is a key factor to reduce the V_{op}. Figure 5 shows the voltage-dependent reflectance and transmittance

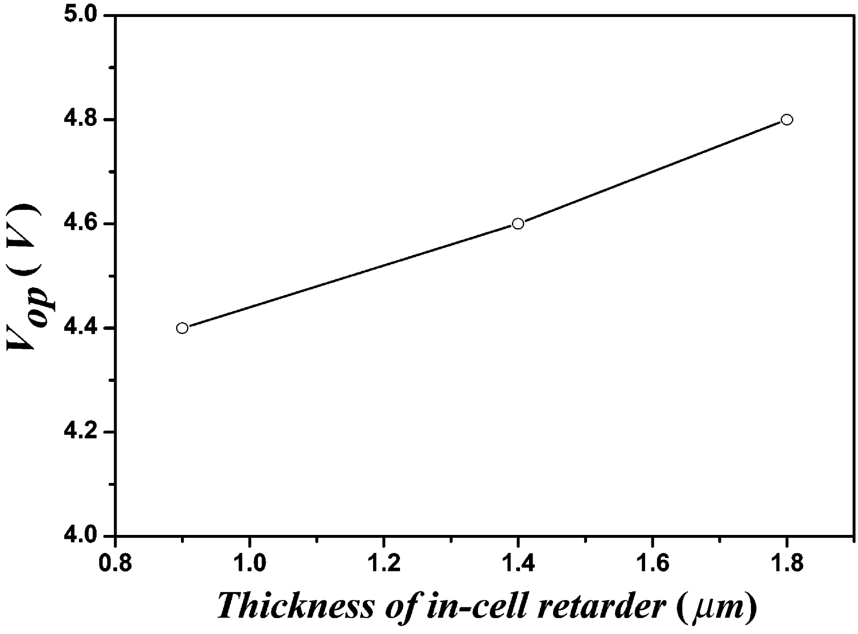

FIGURE 4 Calculated V_{op} as a function of the thickness of the in-cell retarder.

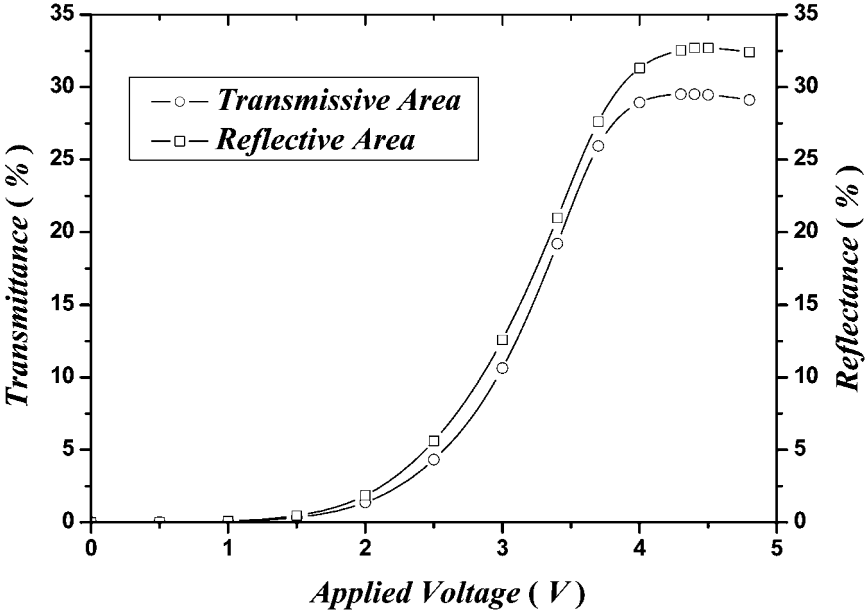

FIGURE 5 Calculated voltage-dependent reflectance and transmittance curves.

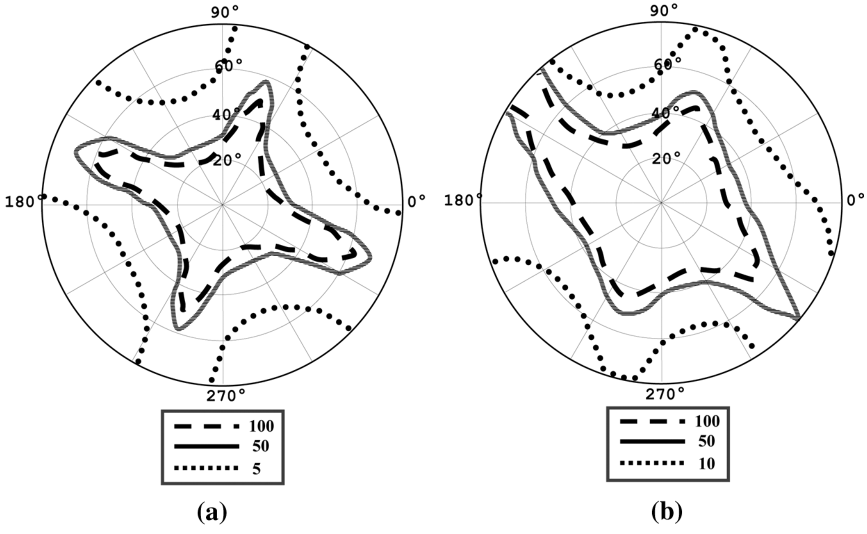

FIGURE 6 Calculated iso-contrast curves at a wavelength of 550 nm for the (a) reflective and (b) transmissive areas.

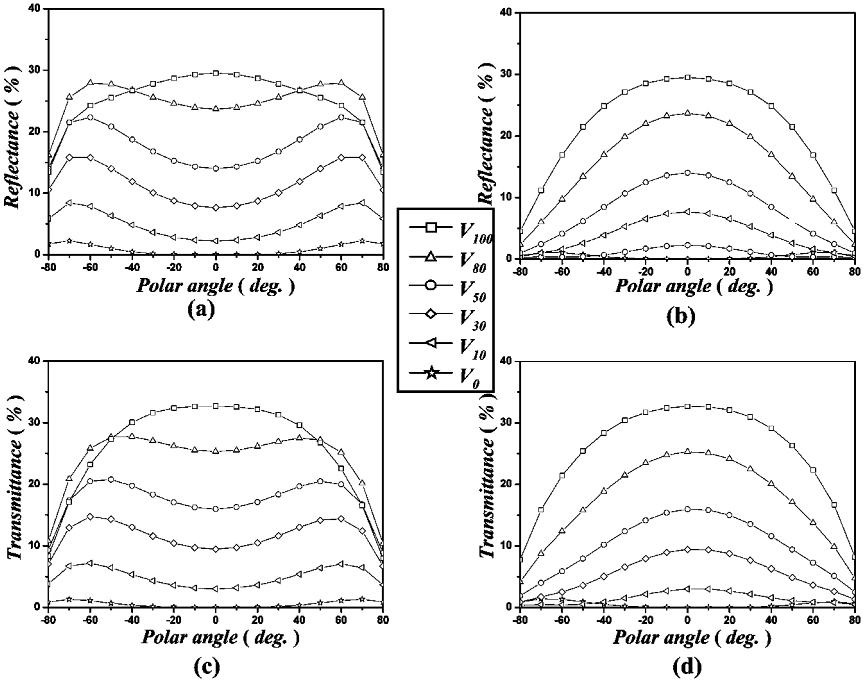

(a) (b) (c) (d)

FIGURE 7 Viewing angle dependence of the 6 grey levels for transflective IPS cell in directions: (a) parallel to the rubbing direction and (b) perpendicular to the rubbing direction in the reflective area, (c) parallel to the rubbing direction and (d) perpendicular to the rubbing direction, perpendicular to the rubbing direction in the transmissive area.

curves in this cell condition. The result shows that the threshold and driving voltages of both the reflective and transmissive area are about the same and thus this display can be displayed with a single driving circuit.

Figure 6 shows the viewing angle characteristics of the proposed cell at 550 nm. In the reflective area, the region in which the contrast ratio (CR) is larger than 5 exists at about 50° of the polar angle in all directions and in the transmissive area, the region in which the CR is large than 10, exists over 50° of the polar angle in all directions. We have also calculated a grey scale inversion for 6 grey levels, which were obtained by dividing the voltage-dependent R and T curves equally in a normal direction. Only data in two directions are shown in Figure 7. In a direction parallel to rubbing direction, both the reflective and transmissive areas do not show grey scale inversion at low gray but appears at a white state {see Figs. 7(a) and 7(c)}. In general, the existence of grey scale inversion at a white state does not deteriorate image quality to an extensive degree. In a direction perpendicular to the rubbing direction, both the transmissive and reflective areas do not show the grey scale inversion up to 45° of the polar angle due to an increase in light leakage of a dark state {see Figs. 7(b) and 7(d)}.

SUMMARY

We have studied electrode structure, cell structure and LC physical properties that affect the electro-optic characteristics of the single gap transflective IPS cell. The device utilizes the electrode surface as a reflective area, and the distance between electrodes as a transmissive area. The results indicate that an optimization of w and l, rubbing angle, thickness of the in-cell retarder and cell retardation value is critical to achieve a cell with high light efficiency, low driving voltage and a single driving circuit. In addition, its electro-optic characteristics depend strongly on the ratio of electrode width to the distance between electrodes. Further, owing to the in-plane orientation of the LC director, the device exhibits a wide viewing angle without the occurrence of a grey scale inversion over a wide range of viewing angles, in both the reflective and transmissive areas, and can be generated with a single driving circuit since the threshold and driving voltages are equal for an optimized cell structure.

REFERENCES

[1] Watanabe, R. & Tomita, O. (2002). *Proc. 9th IDW'02*, 397.
[2] Uesaka, T., Yoda, E., Ogasawara, T., & Toyooka, T. (2002). *Proc. 9th IDW'02*, 417.
[3] Fujimori, K., Narutaki, Y., Itoh, Y., Kimura, N., Mizushima, S., Ishii, Y., & Hijikigawa, M. (2002). *SID'02 Digest*, 1382.
[4] Narutaki, Y., Fujimori, K., Itoh, Y., Shinomiya, T., Kimura, N., Mizushima, S., & Hijikigawa, M. (2002). *Proc. 9th IDW'02*, 299.
[5] Kim, J. C., Jhun, C. G., Park, K. H., Gwag, J. S., Lee, S. H., Lee, G.-D., & Yoon, T.-H. (2003). *Proc. 3rd IMID'03*, 283.
[6] Oh-e, M. & Kondo, K. (1995). *Appl. Phys. Lett.*, *67*, 3895.
[7] Ohmuro, K., Kataoka, S., Sasaki, T., & Koike, Y. (1997). *SID'97 Digest*, 845.
[8] Miyashita, T., Yamaguchi, Y., & Uchida, T. (1995). *Jpn. J. Appl. Phys.*, *34*, 177.
[9] Lee, S. H., Lee, S. L., & Kim, H. Y. (1998). *Appl. Phys. Lett.*, *73*, 2881.
[10] Song, J. H. & Lee, S. H. (2004). *Jpn. J. Appl. Phys.*, *43*, 1130.
[11] Kim, H. Y., Song, I. S., & Lee, S. H. (2003). *Trans. On EEM.*, *4*, 24.
[12] Lien, A. (1990). *Appl. Phys. Lett.*, *57*, 2767.
[13] Song, I. S., Baik, I.-S., Kim, T. M., Lee, S. H., Kim, D. S., Soh, H.-S., & Kim, W. Y. (2004). *Journal of Information Display*, *5*, 18.
[14] Doornkamp, C., van der Zander, B. M. I., Roosendaal, S. J., Stofmeel, L. W. G., van Glabbeek, J. J., Osenga, J. T. M., & Steenbakkers, J. A. M. (2003). *Proc. 10th IDW'03*, 685.